

# Evidence for spin-wave excitations in the long-range magnetically ordered state of a Fe<sub>19</sub> molecular crystal from proton NMR

M. Belesi,<sup>1</sup> F. Borsa,<sup>1,2</sup> and A. K. Powell<sup>3</sup><sup>1</sup>Ames Laboratory—US Department of Energy and Department of Physics and Astronomy, Iowa State University, Ames, Iowa 50011, USA<sup>2</sup>Dipartimento di Fisica “A. Volta”, e Unità CNISM, Università di Pavia, I27100 Pavia, Italy<sup>3</sup>Institute for Inorganic Chemistry, University of Karlsruhe, D76131 Karlsruhe, Germany

(Received 27 June 2006; published 6 November 2006)

We present an investigation of the [Fe<sub>19</sub>(metheidi)<sub>10</sub>(OH)<sub>14</sub>(O)<sub>6</sub>(H<sub>2</sub>O)<sub>12</sub>]NO<sub>3</sub>·24H<sub>2</sub>O (henceforth Fe<sub>19</sub>) high spin magnetic molecular cluster, based on proton NMR measurements obtained in the low temperature regime 0.4–10 K. The onset of a local static field (in the NMR time scale) is observed below about 1 K both in zero external field and with an applied field. In order to discriminate between single molecule spin freezing and the onset of long-range intermolecular magnetic order, as inferred from specific heat measurements [M. Affronte *et al.*, Phys. Rev. B **66**, 064408 (2002)], proton spin-lattice relaxation measurements were performed. For applied fields larger than 0.1 T, the spin-lattice relaxation is driven by the fluctuations of the single molecule magnetization, consistent with a single molecule frozen state. On the other hand, at zero external field, the relaxation rate becomes much faster and it displays, below 1 K, a nearly power law  $T$  dependence, characteristic of nuclear relaxation driven by magnons as expected in the presence of an antiferromagnetic long-range ordered phase. The results are discussed in terms of nuclear relaxation due to Raman two-magnon and three-magnon processes. We find good agreement with the theory for an intermolecular superexchange interaction  $J \approx 1$  mK, while some ambiguity remains about the size of the gap in the spin-wave spectrum.

DOI: 10.1103/PhysRevB.74.184408

PACS number(s): 75.50.Xx, 76.60.-k, 75.75.+a, 75.40.Gb

## I. INTRODUCTION

The strong intramolecular superexchange interactions present in molecular clusters generate magnetic ground states with high total spin values, at low temperatures. Since the intermolecular interactions are relatively weak as compared to the intramolecular ones, these molecular clusters have been widely and predominantly investigated for their single molecule magnetic properties which, in presence of anisotropy, include some remarkable spin dynamical phenomena, such as superparamagnetism and quantum tunneling of the magnetization.<sup>1–7</sup> Recently, there has been a renewed interest in these clusters in view of the possibility of observing the onset of long range magnetic order (LRMO) among the collective molecular spins (arranged in a crystallographic lattice) as driven by weak intermolecular interactions. A phase transition to an ordered state can be realized if the energy scale of the anisotropy is sufficiently small so that the total spins of the molecules do not freeze above the ordering temperature. In clusters with a large anisotropy, such as Mn<sub>12</sub> and Fe<sub>8</sub>, the onset of LRMO is prevented by the single molecule superparamagnetic freezing occurring at relatively high temperatures. On the other hand, there exist a number of clusters with small anisotropy for which the onset of LRMO has been indeed reported: Fe<sub>19</sub>,<sup>8</sup> Mn<sub>4</sub>Br,<sup>9</sup> Mn<sub>4</sub>Me,<sup>10</sup> and Fe<sub>14</sub>.<sup>11</sup> In these systems, the weak intermolecular interactions leading to LRMO appear to be of superexchange nature, while in Mn<sub>6</sub>Br (Ref. 12) and Fe<sub>17</sub> (Ref. 13) it is believed to be purely dipolar.

NMR is a suitable microscopic technique for probing both the local static hyperfine field arising in the LRMO phase through the NMR spectra, and the nature of the collective excitations above such a state through nuclear relaxation measurements. In this paper, we report proton NMR line

shape and spin-lattice relaxation measurements in a Fe<sub>19</sub> polycrystalline sample which confirm the onset of LRMO in zero applied field at  $T \sim 1$  K. The new relevant result here is that our measurements yield information about the magnon band, which appears in the LRMO state.

## II. SAMPLE PROPERTIES AND EXPERIMENTAL DETAILS

The chemical formula of the Fe<sub>19</sub> molecule is [Fe<sub>19</sub>(metheidi)<sub>10</sub>(OH)<sub>14</sub>(O)<sub>6</sub>(H<sub>2</sub>O)<sub>12</sub>]NO<sub>3</sub>·24H<sub>2</sub>O, where the ligand metheidi is N-(1hydroxymethylethyl)imino-diacetic acid, N(CH<sub>2</sub>methylCH<sub>2</sub>OH)(CH<sub>2</sub>CO<sub>2</sub>H)<sub>2</sub>. Details about the synthesis and the structural characterization can be found in Ref. 14. The physics of the ground state  $S=33/2$  manifold of each molecule, can be described by the effective spin Hamiltonian

$$H = g\mu_B \vec{S} \cdot \vec{B}_0 + D \left[ S_z^2 - \frac{1}{3} S(S+1) \right] + E(S_x^2 - S_y^2), \quad (1)$$

where the first term is the Zeeman coupling with the applied magnetic field  $B_0$ , whereas the remaining terms account for the single ion anisotropy. In particular, the anisotropy parameters  $D$  and  $E$  stand for the axial and the rhombic contributions to the zero-field splitting, respectively. Their values are  $D = -0.05$  K and  $E = 0.0072$  K, as obtained by EPR measurements.<sup>14</sup> Hence, neglecting  $E$  and for an applied field  $B_0$  along the main anisotropy axis, the energy levels at low temperatures can be expressed in terms of the quantum number  $m$  as

$$E_m = -0.05(m^2 - 96.25) + 1.33mB_0, \quad (2)$$

where the energy is taken in units of Kelvin, and  $g=2$ . According to Eq. (2), in the  $S=33/2$  manifold, and for zero

field, the energy barrier separating the lowest ( $m = \pm 33/2$ ) from the highest ( $m = \pm 1/2$ ) levels is  $\Delta E = 13.6$  K, whereas the lowest excitation energy is 1.6 K. Thus, in our low temperature measurements, only a few of the low-lying states are thermally populated.

A slow relaxation of the magnetization has been observed in  $\text{Fe}_{19}$  by magnetic measurements with the mean relaxation time following, for  $T > 0.2$  K, an Arrhenius law  $\tau = \tau_0 \times e^{U/k_B T}$ , with energy barrier  $U/k_B = 9.2$  K and attempt time  $\tau_0 = 1.4 \times 10^{-10}$  s, the fastest observed so far in molecular magnets.<sup>8</sup> The relaxation of the magnetization is though relatively fast at low  $T$ , and the system enters a LRMO state (due to the intermolecular interactions) before the superparamagnetic freezing becomes effective. The transition to a LRMO, at  $T_N = 1.19$  K, has been inferred from a lambda anomaly in the specific heat measurements while the low  $T$  magnetization measurements suggest an antiferromagnetic (AFM) ordering of the magnetic moments that is attributed to weak superexchange interactions between the adjacent  $\text{Fe}_{19}$  molecules.<sup>8</sup>

We have performed  $^1\text{H}$  NMR measurements in a polycrystalline  $\text{Fe}_{19}$  sample with a TecMag fourier transform (FT) pulse spectrometer. The proton NMR spectra were acquired by sweeping the external magnetic field while keeping the irradiation frequency constant. The echo was obtained by a standard Hahn echo pulse sequence with a typical  $\pi/2$  pulse length of  $3 \mu\text{s}$ , with the separation between the pulses being  $10\text{--}15 \mu\text{s}$  depending on the experimental conditions. The  $^1\text{H}$  spin-lattice relaxation  $T_1^{-1}$  rate was measured at the center of the spectrum by monitoring the recovery of the nuclear magnetization following a saturating comb of  $rf$  pulses. The recovery of the nuclear magnetization was found to be nonexponential (stretched exponential) in the whole temperature range due to the distribution of relaxation rates of the different protons sites in the cluster. The  $T_1^{-1}$  values reported here were calculated by fitting the data at each  $T$  by a stretched exponential function. The experiments were carried out in the temperature range  $0.4\text{--}10$  K using (i) a continuous flow cryostat ( $T > 4$  K), (ii) a bath cryostat ( $1.4\text{--}4.2$  K), and (iii) a closed cycle  $\text{He}_3$  cryostat ( $T < 2$  K).

### III. EXPERIMENTAL RESULTS AND DISCUSSION

The temperature evolution of the  $^1\text{H}$  NMR spectra at low temperatures ( $T < 2$  K) is presented in Figs. 1 and 2, for two different irradiation frequencies, 5.81 MHz and 8.085 MHz, respectively. From the high temperature region (not shown) down to 1 K, the spectra consist of a single symmetric line whose width progressively increases by decreasing temperature in a way proportional to the magnetic susceptibility.<sup>15</sup> The behavior is typical of an inhomogeneously broadened line where the overall width of the spectrum is proportional to the local magnetic moment. A different behavior is observed for  $T < 0.8$  K where the spectrum abruptly becomes strongly asymmetric and broad (see Figs. 1 and 2).

Another important feature of the proton NMR in  $\text{Fe}_{19}$  is that the signal intensity of the integrated spectrum decreases drastically in an intermediate temperature regime indicating the loss of nuclei from the observed resonance line (wipeout

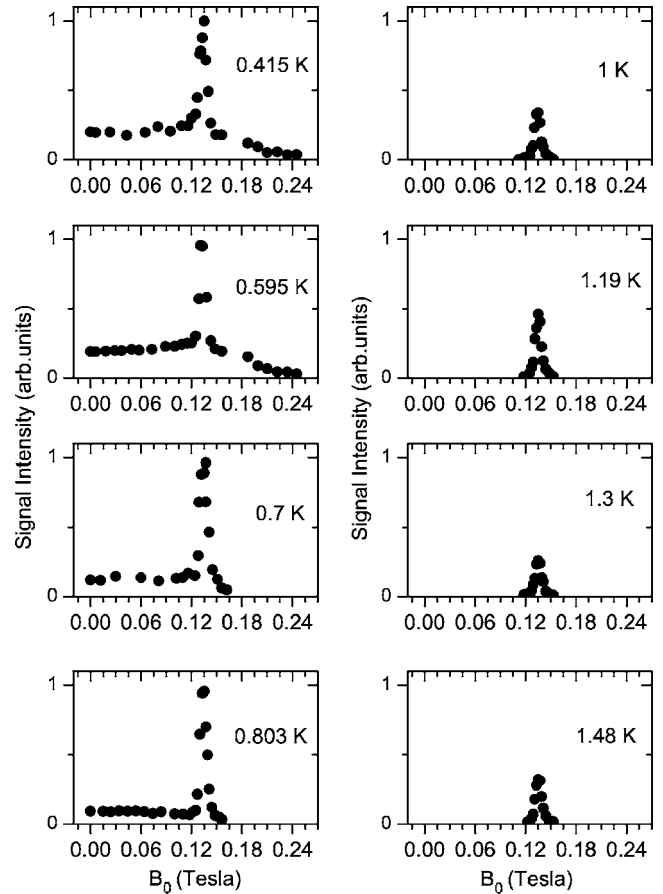


FIG. 1.  $^1\text{H}$  NMR spectra in  $\text{Fe}_{19}$  as measured at constant irradiation frequency  $\nu_L = 5.810$  MHz and for  $T < 1.5$  K.

effect). This effect was thoroughly studied in Ref. 15 from room temperature down to 4 K for a series of single molecule magnets (SMM's) including  $\text{Fe}_{19}$ . The wipeout of the proton NMR signal intensity that takes place in the intermediate temperature range was shown to arise from the coupling of nuclear spins with slow fluctuating degrees of freedom, i.e., the exchange coupled magnetic ions within each molecule. By lowering the temperature, the electronic spin correlation time  $\tau_c(T)$  (which describes the dynamics of the exchanged coupled magnetic ions) gets longer and the spin-spin relaxation rate  $T_2^{-1}$  that varies as  $T_2^{-1} \sim \tau_c(T)$  (fast motion approximation),<sup>16</sup> becomes so fast that the nuclei relax before they can be observed in a NMR experiment (wipeout effect). At a given temperature, denoted here by  $T_f$ , the correlation time  $\tau_c(T)$  becomes so long that  $\tau_c \gamma h_L \sim 1$  (where  $h_L$  denotes the fluctuating local field), and the motional narrowing limit breaks down. Below  $T_f$ , the local field  $h_L$  becomes static in the time scale of the Larmor precession period in the local field itself. As a consequence, the line broadens inhomogeneously, the  $T_2$  increases again towards the value corresponding to nuclear dipolar interactions, and the NMR signal intensity recovers, as can be observed in Figs. 1 and 2.

It must be pointed out that the relaxation measurements reported in the present paper refer to the low temperature regime, where the signal intensity is recovering its full intensity. Because of the width of the line, many  $T_1^{-1}$  measure-

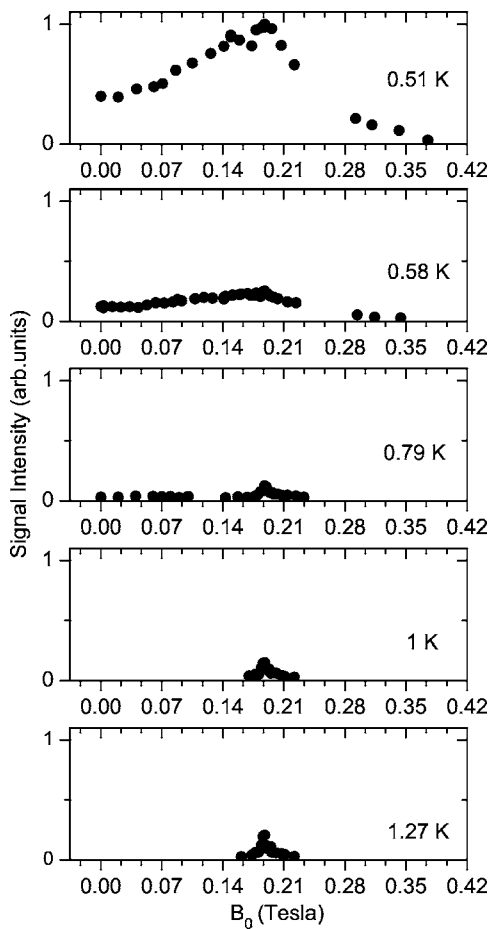


FIG. 2.  $^1\text{H}$  NMR spectra in  $\text{Fe}_{19}$  as measured in the low temperature regime for irradiation frequency  $\nu_L=8.085$  MHz.

ments presented here refer only to a part of the spectrum. However, in the absence of the wipeout effect the results should be representative of an average of all nuclei in the sample. The appearance of a broad distribution of static local internal fields at the proton sites is a result of the frozen  $\text{Fe}^{3+}$  spin configuration in the high spin ground state. A frozen spin configuration in the time scale of the interaction energy  $[(\gamma h_L)^{-1} \approx 3 \times 10^{-8}$  s, see Figs. 1 and 2] is in relatively good agreement with the relaxation time of the magnetization which yields  $\tau=4 \times 10^{-6}$  s, at  $T \sim 0.8$  K.<sup>8</sup>

The onset of a static local field at the proton sites at low  $T$ , is supported by the appearance of a weak zero field proton NMR signal which can be observed in a broad frequency range,  $\nu_L \sim (5-21)$  MHz. This signal appears around 1 K, as measured for different irradiation frequencies [see Fig. 3(a)]. A static local field at the proton site is expected once the  $\text{Fe}^{3+}$  magnetic moments are in a frozen spin configuration. If this configuration is due to the superparamagnetic blocking, the molecular spins freeze along the direction dictated by the magnetic anisotropy. Alternatively, if the intermolecular interactions are strong enough, the neighboring molecular spins are correlated and the system can be stabilized in a LRMO state. The discrimination between these two physically different phases (i.e., superparamagnetic blocking vs LRMO) is not possible with a static NMR experiment at zero field, as both scenarios are equally supported by the presence

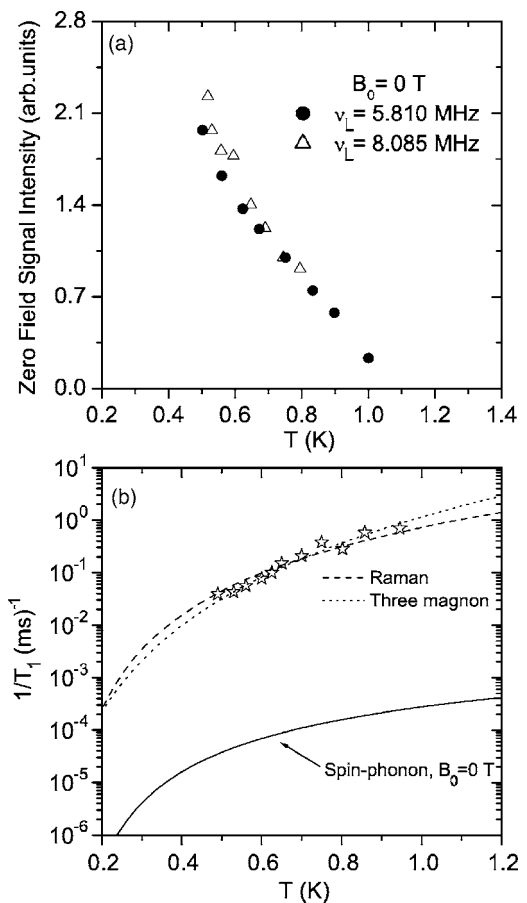


FIG. 3. (a) Zero field  $^1\text{H}$  NMR intensity as measured at two different irradiation frequencies,  $\nu_L=5.81$  MHz ( $\bullet$ ) and  $\nu_L=8.085$  MHz ( $\Delta$ ). (b)  $^1\text{H}$  spin-lattice relaxation rate  $T_1^{-1}$  data ( $\star$ ) vs temperature measured at zero external field and for irradiation frequency  $\nu_L=5.81$  MHz. The dashed and the dotted lines are the best fit to the data with Eq. (7) for  $J=1.3 \pm 0.2$  mK, and Eq. (8) for  $J=1.2 \pm 0.2$  mK, respectively. For comparison purposes, we also plot (solid line) the expected temperature dependence of  $T_1^{-1}$  according to Eq. (4), for zero external field and at the resonance frequency corresponding to a local internal field  $h_L=0.2$  T. The onset of a signal intensity at zero field at about 1 K in part (a), combined with the NSLR data in part (b) is a strong indication for a LRMO state.

of a zero field signal. On the other hand, a thorough study of the nuclear spin-lattice relaxation mechanism can shed light on the nature of the low- $T$  magnetic state, since the excitation spectrum and hence the spin dynamics should be quite different for a LRMO state and a single spin frozen state.

Our experimental results for the nuclear spin-lattice relaxation rate (NSLR)  $T_1^{-1}$  are presented in Figs. 3(b) and 4. These data were acquired for (i) three different values of the external magnetic field (always higher than 0.12 T) and for a temperature range where the signal intensity starts to recover (Fig. 4), and (ii) at zero external field and for irradiation frequency of  $\nu_L=5.81$  MHz [Figs. 3(b) and 4]. The most striking experimental result is the spectacular effect of the external magnetic field, on the magnitude and the temperature dependence of the NSLR. The zero field NSLR is strongly temperature dependent and its value is enhanced by three orders of magnitude as compared with the correspond-

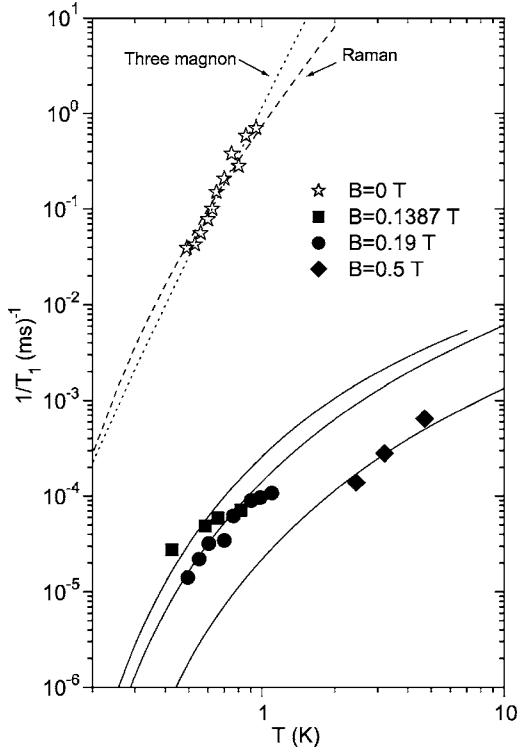


FIG. 4.  $^1\text{H}$  spin-lattice relaxation rate  $T_1^{-1}$  vs temperature as measured at zero external field for an irradiation frequency  $\nu_L = 5.81$  MHz together with data at different external fields at the corresponding Larmor frequencies. The solid lines are the fits according to Eq. (4), the dashed line is the fit to the zero field data from Raman processes [Eq. (7)] whereas the dotted line is the expected temperature dependence from three-magnon relaxation processes [Eq. (8)].

ing rate in the presence of small applied fields (e.g., at 0.138 T). This remarkable change in the spin dynamics is strongly indicative of the presence of a relaxation mechanism at  $B_0 = 0$  T which is drastically different from the one operating at the given finite fields ( $B_0 > 0.13$  T). We propose that our NSLR data can be explained (see below) by the presence of collective spin-waves excitations in a LRMO state at  $B_0 = 0$  T. As mentioned above, this scenario is supported by magnetic and specific heat measurements showing the onset of an ordered state at  $T_N \sim 1.19$  K for  $B_0 = 0$  T, which remains stable only for very low values of the external field, namely for  $B_0 < 0.12$  T,<sup>8</sup> for higher fields a single molecule superparamagnetic state is stabilized.

#### A. Nuclear spin-lattice relaxation for $B_0 > 0.13$ T: The superparamagnetic phase

The NSLR data presented here for  $B_0 > 0.13$  T refer to a temperature and field range in which the superparamagnetic blocking is effective; the temperatures considered are such that most of the molecules are in their high spin  $S = 33/2$  manifold, and the applied fields are low enough so that the anisotropy barrier is not drastically modified. The NSLR can thus be attributed to the fluctuations of the  $\text{Fe}^{3+}$  magnetic ions due to intrawell transitions.<sup>17,18</sup> The NSLR can be ex-

pressed in terms of the spectral density of the transverse component of the local (i.e., at the proton sites) hyperfine field  $h_{\pm}(t)$ , evaluated at the proton Larmor frequency  $\omega_L$ . As explained in Refs. 17 and 18, this spectral density can be approximated with the corresponding one of the orientation of the total magnetization of the molecular cluster. In turn, the latter is driven by the irreversible decay of the spin correlations due to the spin-phonon coupling and this can be described phenomenologically by introducing the lifetime broadening parameters  $1/\tau_m$  (given below) for each sublevel  $m$ . This gives, for the NSLR,<sup>17,18</sup>

$$\frac{1}{T_1} = \frac{A}{Z} \sum_m \frac{\tau_m \exp(-E_m/k_B T)}{1 + \omega_L^2 \tau_m^2}, \quad (3)$$

where  $Z$  is the partition function,  $\gamma_N$  is the nuclear gyromagnetic ratio,  $\omega_L$  is the Larmor frequency, and  $A$  is the average of the square of the hyperfine interaction energy. The energy eigenvalues  $E_m$ , are given by Eq. (2), while the parameters  $\tau_m$  of the individual  $m$  sublevels can be expressed in terms of the spin-phonon transition rates  $W$  from  $m$  to  $m \pm 1$ , and  $m \pm 2$  as follows<sup>19</sup>

$$\tau_m^{-1} = W_{m \rightarrow m+1} + W_{m \rightarrow m-1} + W_{m \rightarrow m+2} + W_{m \rightarrow m-2}, \quad (4)$$

with

$$W_{m \rightarrow m \pm 1} = C' s_{\pm 1} \frac{(E_{m \pm 1} - E_m)^3}{\exp[\beta(E_{m \pm 1} - E_m)] - 1}$$

$$W_{m \rightarrow m \pm 2} = 1.06 C' s_{\pm 2} \frac{(E_{m \pm 2} - E_m)^3}{\exp[\beta(E_{m \pm 2} - E_m)] - 1}, \quad (5)$$

where  $s_{\pm 1} \equiv (s \mp m)(s \pm m + 1)(2m + 1)^2$ , and  $s_{\pm 2} \equiv (s \mp m)(s \pm m + 1)(s \mp m - 1)(s \pm m + 2)$ . Here  $C' \equiv D'^2 / (12\pi\rho u^5 \hbar^4)$ , where  $\rho$  denotes the mass density,  $u$  the sound velocity, and  $D'$  the spin-phonon coupling constant which is related to the axial anisotropy constant  $D$  in Eq. (1).<sup>19</sup> In the slow motion regime, ( $\tau_m \omega_L \gg 1$ ), which is relevant at low temperatures, the parameters  $A$  and  $C'$  appear in Eq. (3) only as a product,  $AC'$ .

The optimal fit to our data, according to Eqs. (3)–(5), is shown in Fig. 4 (solid lines) and provides us with the product  $AC' = 4 \times 10^9$  rad/s<sup>3</sup> K<sup>3</sup>. This value is three orders of magnitude smaller than the corresponding one in  $\text{Mn}_{12}$  (Ref. 17) and four orders of magnitude smaller than in  $\text{Fe}_8$ .<sup>18</sup> Since, in molecular nanomagnets, the hyperfine parameter  $A$  for protons takes values in the range  $10^{12}$ – $10^{13}$  rad/s<sup>2</sup> (Refs. 17, 18, and 20) the main source of difference among the three different clusters is to be attributed to the spin-phonon coupling constant  $C'$ . A smaller value of  $C'$  in  $\text{Fe}_{19}$  is consistent with the smaller value of the anisotropy constant  $D'$  in  $\text{Fe}_{19}$  with respect to the other two clusters. It should also be noted that the value of  $C'$  is very sensitive to the elastic properties of the molecule via the sound velocity parameter  $u$ .

#### B. Nuclear spin-lattice relaxation at $B_0 = 0$ T: The LRMO phase

As we pointed out above, the nuclear spin-lattice relaxation mechanism is severely affected by the presence of the



magnetic field. The fact that the NSLR below 1 K (Fig. 4) increases by more than three orders of magnitude when the external field is reduced to zero from the low value of 0.13 T indicates a dramatic change in the excitation spectrum as one would expect if the system develops long-range magnetic order and collective excitations. As we show below, this drastic increase in the nuclear relaxation rate and its strong temperature dependence are clear signatures of relaxation due to scattering with magnons. In particular, the nuclear spin-lattice relaxation in ordered magnetic insulators arises via the hyperfine interaction, when a nuclear spin directly interacts with one or more spin waves. First and second order scattering processes involving one, two, and three magnons have been treated in detail in Ref. 21. We will consider here only the more important first order processes. The direct relaxation process involving a nuclear spin flip accompanied by the creation of a spin wave should be negligible in an AFM ordered state due to the difficulty to satisfy energy conservation even in the presence of a small gap in the spin-wave spectrum. The two-magnon Raman process does not present this difficulty although it requires an anisotropic hyperfine interaction in order to satisfy the conservation of angular momentum. Since the hyperfine interaction of protons with the  $\text{Fe}^{3+}$  is predominantly of dipolar origin, the Raman process should be significant here. The expression for the corresponding nuclear relaxation rate is:<sup>21</sup>

$$\frac{1}{T_1} = \frac{A^2}{\hbar^2 \omega_e} \frac{8 \sin^2 \theta}{(2\pi)^3 b^6} \left( \frac{k_B T}{\hbar \omega_e} \right)^3 \int_{T_{AE}/T}^{\infty} \frac{xdx}{e^x - 1}, \quad (6)$$

where  $T_{AE}$  is given in terms of the  $\omega_{AE}$ , as  $T_{AE} = \frac{\hbar \omega_{AE}}{k_B}$ ; also  $\hbar \omega_e = 2JzS$ , where  $J$  is the intermolecular exchange interaction and  $z$  is the number of nearest neighbor molecules. The parameter  $b$  is defined as  $b^2 \equiv 2/z$  and  $\theta$  denotes the angle between the local hyperfine field at the nuclear site and the anisotropy axis, which is the quantization direction for the electronic spins. The angle  $\theta$  can be different from zero only for dipolar hyperfine interaction. In order to fit the data with Eq. (6), we set the values of the parameters that are approximately known to reduce the fitting parameters to only two, i.e.,  $J$  and  $T_{AE}$ . Thus, by choosing for the average dipolar hyperfine interaction  $(A/\hbar)^2 = 10^{12} \text{ rad s}^{-2}$ ,<sup>17,18,20</sup>  $z=6$  and  $\sin^2 \theta = 0.5$  (i.e., by considering an average over all angles) one has

$$\frac{1}{T_1} = 2.2 \times 10^{-9} \frac{T^3}{J^4} I_2(T_{AE}/T), \quad (7)$$

where  $I_2(T_{AE}/T)$  is the Debye integral and  $J$  is expressed in units of temperature. As shown by the dashed line in Figs. 3(b) and 4 a satisfactory fit of the data can be obtained by choosing  $T_{AE} = 1 \text{ K}$  and  $J = 1.3 \text{ mK}$ . These values should be considered with an uncertainty of about 20% in view of the limited temperature range of the experimental data.

Besides the Raman process described above, the three-magnon processes can also contribute to the nuclear relaxation<sup>21</sup> and should thus be considered also in our case. For example, in canted antiferromagnets such as  $\text{KMnF}_3$ , a  $T^5$  law has been detected experimentally<sup>22</sup> and justified theoretically in terms of three-magnon processes. The contribu-

tion to the NSLR from the three-magnon processes for AFM insulators, as derived by Beeman and Pincus,<sup>21</sup> is given by

$$\frac{1}{T_1} = \left( \frac{A^2}{\hbar^2 \omega_e} \right) \left[ \frac{5}{S(2\pi)^5 b^9} \right] \left( \frac{k_B T}{\hbar \omega_e} \right)^5 I_3 \left( \frac{\hbar \omega_{AE}}{k_B T} \right) \quad (8)$$

Here,  $S$  is the total spin and  $I_3(\hbar \omega_{AE}/k_B T)$  is a temperature dependent integral.<sup>21</sup> Choosing, as above,  $(A/\hbar)^2 = 10^{12} \text{ rad s}^{-2}$  and  $z=6$ , the data can also be fitted [dotted line in Figs. 3(b) and Fig. 4] by the three magnon process for  $T_{AE} = 0.1 \text{ K}$  and  $J = 1.2 \text{ mK}$ .

We conclude that both the Raman and the three-magnon processes can account for the size and  $T$  dependence of the nuclear relaxation in the LRMO phase. In the first case, one would estimate a gap  $T_{AE} = 1 \pm 0.1 \text{ K}$  and an intermolecular interaction  $J = 1.3 \pm 0.2 \text{ mK}$ , while in the second case, we have  $T_{AE} = 0.1 \text{ K}$  and  $J = 1.2 \pm 0.2 \text{ mK}$ . Unfortunately, based on the available experimental data, it is not possible to distinguish between the two possible relaxation mechanisms or their relative contributions to the nuclear relaxation process. Correspondingly, the remaining uncertainty in the size of the spin wave gap could be resolved by nuclear relaxation measurements at ultra low temperatures ( $T < 100 \text{ mK}$ ).

#### IV. SUMMARY AND CONCLUSIONS

We have carried out a detailed  $^1\text{H}$  NMR study of the static and dynamic properties of the  $\text{Fe}_{19}$  molecular magnet at low temperatures. The proton NMR spectra (Figs. 1 and 2) for  $T < 2 \text{ K}$  gain rapidly in intensity, and for  $T_f \sim 0.8 \text{ K}$  a broad distribution of static local internal fields is observed. This behavior is indicative of the ‘‘freezing’’ of the  $\text{Fe}^{3+}$  magnetic moments, in the NMR time scale, as the system condensates in its high spin ground state of  $S = 33/2$ . We notice here that the signal shown in Figs. 1 and 2 arises mainly from the local fields in the frozen superparamagnetic phase given that the signal from the LRMO phase is only the low intensity signal observed for  $B < 0.1 \text{ T}$ . Since no discontinuity is observed in Figs. 1 and 2 going from  $B = 0$  to  $B = 0.1 \text{ T}$ , the field above which the LRMO appears to disappear,<sup>8</sup> one draws the conclusion that the internal field is almost the same in the frozen state and in the LRMO state.

A frozen spin configuration in this temperature range is also supported by magnetization relaxation data.<sup>8</sup> The  $^1\text{H}$  NSLR data reported here for  $B > 0.1387 \text{ T}$  and at low  $T$  (where the molecules are in their high spin magnetic state), can be explained in terms of a phenomenological model<sup>17,18</sup> whereby the NSLR is attributed to the fluctuations of the  $\text{Fe}^{3+}$  magnetic moments due to intrawell transitions triggered by the spin-phonon interactions. The spin-phonon coupling constant obtained from the NSLR data is very small compared to the ones found in the  $\text{Mn}_{12}$  and  $\text{Fe}_8$  clusters, which can be expected since the value of the anisotropy constant  $D$  is very small in  $\text{Fe}_{19}$ .

The new relevant experimental result of the present study is the drastic effect of the external magnetic field, on the magnitude and temperature dependence of the NSLR. In particular, as the external field decreases from 0.1387 T down to zero, the NSLR increases by three orders of magnitude. This

behavior reveals a significant modification of the excitation spectrum, which is attributed to the stabilization of a long-range magnetic ordered state for external magnetic field  $B_0 < 0.13$  T. In the LRMO state the gap between the single molecule ground state and the first excited state, which is responsible for the very long nuclear relaxation time in the superparamagnetic phase, becomes filled with a continuum of magnon states. Our interpretation is in agreement with magnetization and specific heat measurements which show the onset of an AFM state for  $B_0 < 0.12$  T.<sup>8</sup>

The nuclear relaxation rate in the LRMO state can be explained both in terms of Raman and/or three-magnon processes according to the theoretical formulas of Beeman and Pincus,<sup>21</sup> both providing an estimate of the exchange parameter  $J$  to be of the order of  $J \approx 1$  mK, consistent with the  $J$  value estimated from the Weiss temperature  $\theta = -1.7$  K,<sup>8</sup> under the assumption of an isotropic Heisenberg AFM Hamiltonian. However, one is not able to infer on the relative contributions of each of the two processes and thus the exact value of the spin wave gap remains ambiguous.

The small value of the intermolecular exchange constant  $J$ , is anticipated in molecular crystals since intercluster interactions are generally very weak and accordingly manifest their existence only at very low  $T$ . A superexchange interaction between neighbor magnetic molecules, mediated via water of crystallization and coordinated water, or uncoordinated oxygen atoms of the ligands on the outer ions of the cluster, has been argued to be responsible for the AFM long range magnetic ordering.<sup>8</sup> In contrast, the strength of the dipolar

interactions between adjacent molecules,  $E_{\text{dip}} \sim 190$  mK, is considered to be relatively weak for an AFM transition observed at  $T_N \sim 1.19$  K.<sup>8</sup>

Regarding the spin-wave gap, the theoretical prediction based on calculations in Heisenberg antiferromagnets with single ion easy axis anisotropy<sup>23</sup> yields  $\Delta(B=0) = 2S\sqrt{D^2 + zDJ}$ . In the present case of  $\text{Fe}_{19}$  in the LRMO state, with  $D = -0.05$  K,  $J = 1$  mK,  $S = 33/2$ , and  $z = 6$ , one has  $\Delta(B=0) = 1.74$  K. The prediction seems to favor the fit of the data with the two-magnons Raman process in Figs. 3(b) and 4 (see Eq. (6) which yields a gap value of about 1 K.

More details about the spin wave spectrum and its gap could be obtained by neutron scattering measurements and very low temperature nuclear relaxation measurements. The study of spin waves in  $\text{Fe}_{19}$  could unveil new physics in view of the unusual situation of having large spins ( $S = 33/2$ ) interacting via an exchange interaction much smaller ( $J \approx 1$  mK) than the zero field crystal field splitting ( $D = -0.05$  K).

We would like to acknowledge the able experimental assistance of R. Vincent and useful discussions with A. Lascialfari, P. Carretta, and I. Rousochatzakis. We also thank Jin-Kui Tang for preparing the ligand and the crystals of  $\text{Fe}_{19}$ . Ames Laboratory is operated for the U.S. Department of Energy by Iowa State University under Contract No. W-7405-Eng-82. The work in Pavia was supported in part by the NOE-MAGMANET European program.

- 
- <sup>1</sup>D. Gatteschi, A. Caneschi, L. Pardi, and R. Sessoli, *Science* **265**, 1055 (1994).
- <sup>2</sup>O. Kahn, *Molecular Magnetism* (VCH, Berlin, 1990).
- <sup>3</sup>R. Sessoli, D. Gatteschi, A. Caneschi, and M. A. Novak, *Nature (London)* **365**, 141 (1993).
- <sup>4</sup>J. R. Friedman, M. P. Sarachik, J. Tejada, J. Maciejewski, and R. Ziolo, *J. Appl. Phys.* **79**, 6031 (1996).
- <sup>5</sup>J. R. Friedman, M. P. Sarachik, J. Tejada, and R. Ziolo, *Phys. Rev. Lett.* **76**, 3830 (1996).
- <sup>6</sup>L. Thomas, F. Lioni, R. Ballou, D. Gatteschi, R. Sessoli, and B. Barbara, *Nature (London)* **383**, 145 (1996).
- <sup>7</sup>D. Gatteschi and R. Sessoli, *Angew. Chem., Int. Ed.* **42**, 268 (2003).
- <sup>8</sup>M. Affronte, J. C. Lasjaunias, W. Wernsdorfer, R. Sessoli, D. Gatteschi, S. L. Heath, A. Fort, and A. Rettori, *Phys. Rev. B* **66**, 064408 (2002).
- <sup>9</sup>A. Yamaguchi, N. Kusumi, H. Ishimoto, H. Mitamura, T. Goto, N. Mori, M. Nakano, K. Awaga, J. Yoo, J. Hendrickson, and G. Christou, *J. Phys. Soc. Jpn.* **71**, 414 (2002).
- <sup>10</sup>M. Evangelisti, F. Luis, F. L. Mettes, N. Aliaga, G. Aromi, J. J. Alonso, G. Christou, and L. J. de Jongh, *Phys. Rev. Lett.* **93**, 117202 (2004).
- <sup>11</sup>M. Evangelisti, A. Candini, A. Ghirri, M. Affronte, E. K. Brechin, and E. J. L. McInnes, *Appl. Phys. Lett.* **87**, 072504 (2005).
- <sup>12</sup>A. Morello, F. L. Mettes, F. Luis, J. F. Fernandez, J. Krzystek, G. Aromi, G. Christou, and L. J. de Jongh, *Phys. Rev. Lett.* **90**, 017206 (2003).
- <sup>13</sup>M. Evangelisti *et al.* (unpublished).
- <sup>14</sup>J. C. Goodwin, R. Sessoli, D. Gatteschi, W. Wernsdorfer, A. K. Powell, A. K. Powell, and S. L. Heath, *J. Chem. Soc. Dalton Trans.* 2000, 1835.
- <sup>15</sup>M. Belesi, A. Lascialfari, D. Procissi, Z. H. Jang, and F. Borsa, *Phys. Rev. B* **72**, 014440 (2005).
- <sup>16</sup>C. P. Slichter, *Principles of Magnetic Resonance* (Springer-Verlag, New York, 1996).
- <sup>17</sup>A. Lascialfari, Z. H. Jang, F. Borsa, P. Carretta, and D. Gatteschi, *Phys. Rev. Lett.* **81**, 3773 (1998).
- <sup>18</sup>Y. Furukawa, K. Kumagai, A. Lascialfari, S. Aldrovandi, F. Borsa, R. Sessoli, and D. Gatteschi, *Phys. Rev. B* **64**, 094439 (2001).
- <sup>19</sup>J. Villain, F. Hartman-Boutron, R. Sessoli, and A. Rettori, *Europhys. Lett.* **27**, 537 (1994); F. Hartman-Boutron, P. Politi, and J. Villain, *Int. J. Mod. Phys. B* **10**, 2577 (1996); M. N. Leuenberger and D. Loss, *Phys. Rev. B* **61**, 1286 (2000).
- <sup>20</sup>A. Cornia, A. Fort, M. G. Pini, and A. Rettori, *Europhys. Lett.* **50**, 88 (2000).
- <sup>21</sup>D. Beeman and P. Pincus, *Phys. Rev.* **166**, 359 (1968).
- <sup>22</sup>R. J. Mahler, A. C. Daniel, and P. T. Parrish, *Phys. Rev. Lett.* **19**, 85 (1967).
- <sup>23</sup>S. W. Lovesey, *Theory of Neutron Scattering in Condensed Matter* (Clarendon, Oxford, 1984), Vol. 2.